Characterization of nanostructured ceramic and cermet coatings deposited by plasma spraying

E. Sánchez (1), E. Bannier (1), M. Vicent (1), A. Moreno (1), M.D. Salvador (2), V. Bonache (2), E. Klyatskina (2), A. R. Boccaccini (3)

(1) Instituto de Tecnología Cerámica - Asociación de Investigación de las Industrias Cerámicas. Universitat Jaume I. Castellón, Spain.

(2) Instituto de Tecnología de Materiales. Universidad Politécnica de Valencia. Valencia, Spain.

(3) Department of Materials. Imperial College London, London SW7 2BP, UK

Contact e-mail: emilie.bannier@itc.uji.es

ABSTRACT

Industry has a growing need of advanced coatings for a variety of applications (aerospace, special machinery, medicine …). Nanostructured coatings have the potential of providing novel materials with enhanced properties. This paper describes the results of recent research on wear resistant nanostructured coatings. Cermet (WC-Co) and ceramic (Al_2O_3-TiO_2) coatings were obtained by atmospheric plasma spraying. Coating microstructure and phase composition were characterized using SEM, EDX and XRD techniques. Vickers microhardness (HV) of the coatings was also measured. The microstructure and properties of the developed nanostructured coating was compared with those of their conventional counterparts. The influence of the substrate on both microstructure end properties was investigated, as the coatings were deposited on two different steels. In the WC-Co coatings, significant decomposition of the WC particles occurred during spraying which is prejudicial to wear resistance. Nanostructured Al_2O_3-TiO_2 coatings exhibited a bimodal microstructure that retained

the initial nanostructure of the powder. The presence of these areas leads to better tribological properties.

1. Introduction

Advanced coatings are needed in many industrial sectors to enhance the surface characteristics of structural elements or to functionalize a surface. In the former case, the purpose is usually to improve some given material's properties in order to provide protection against wear, corrosion, chemical attack, thermal shock and/or high temperatures. In the latter case, the coating provides a surface with a new function, such as self-lubricating, catalytic, bioactive or self-cleaning coatings. Much research has been undertaken into nanostructured materials, which generally display better physical or mechanical properties than their conventional counterparts [1,2]. As a result, nanostructured coatings could lead to significant advances in the availability of high-performance materials in various industrial sectors [3,4].

There are numerous techniques for producing coatings: physical vapour deposition, chemical vapour deposition, thermal spraying, electrochemical techniques, sol-gel methods. Among these techniques, thermal spraying is one of the most versatile for depositing thick coatings. In such process, a feed material is fused and accelerated until it impacts upon the substrate, where it is rapidly cooled, forming the coating [5]. ~~(figure 1). Thermal spray techniques can be classified in two large families, depending on whether the energy source is of chemical or electric origin (figure 2) [5]. The different techniques differ in flame temperature and particles velocity.~~

The two most commonly used thermal spray methods are atmospheric plasma spraying (APS) and high velocity oxy-fuel flame spraying (HVOF), in which the feed material is in powder form [6]. As a result, in order to obtain nanostructured coatings using these techniques, it should be convenient to use nanoparticles as raw material. However nanoparticles cannot be sprayed directly owing to their small mass. Thus

sprayable nanostructured powders must be obtained in two stages [7,8]. First, the nanoparticles need to be synthesised. Then, they have to be agglomerated to form sprayable micrometric aglomerates. This second stage, which is critical for the success of the method, is known as reconstitution process.

Innumerable methods exist to produce nanoparticles [9-13] but spray drying is the most widespread process for reconstituting nanoparticles into appropriate micrometric granules for thermal spray deposition [7,14-16]. The process consists, basically, of spraying a suspension through a nozzle into a drying chamber where the solvent is removed, producing a highly flowable agglomerate powder as a result of the sphericity of the agglomerates.

It is important to point out that not all spray-dried powders are suitable for thermal spray coatings. The reconstituted powder must be dense enough and have a proper size distribution. A fine and porous powder can not be fed adecuatly into the flame, conducing to low deposition efficiency, poor adhesion and high coating porosity. Some researchers [17] have found that spray-dried powders with bulk density $>1.7 \times 10^3$ kg/m^3 and mean particle size > 20 μm can be directly used for plasma spray coating.

Once the reconstituted nanometric powder has been obtained, the process parameters need to be adapted to the characteristics of the new powder. In particular, heating of the agglomerates need to be closely controlled in order to preserve the nanostructure in the final coating without impairing adhesion to the substrate [18,19]. An intense research activity is being developed during this decade which deals with nanostructured powders to obtain different types of oxide and non-oxide coatings, such as alumina [20], titania [21,22], alumina-titania [23-25], stabilized zirconia [26-28], and cermets [23-31].

In this work alumina-titania ceramic coatings and cemented tungsten carbide cermet coatings were obtained by APS using commercial conventional micrometric powders and reconstituted nanopowders. Both materials are commonly used to form wear-

resistant coatings on metallic substrates and the use of nanostructured feedstock is expected to enhance their properties. This study is aimed to characterize the microstructure of the developed nanostructured coating and to compare the results with those of their conventional counterparts. Vickers microhardness (HV) of the coatings was also measured, as it is a highly relevant property of wear-resistant coatings. The influence of the substrate on both microstructure and properties was also investigated, as the coatings were deposited on two different steels.

2. Experimental techniques

2.1. Materials

Cermet (WC-Co) and ceramic (Al_2O_3-TiO_2) coatings were sprayed using commercial (conventional and nanostructured) thermal spray powders. The characteristics of the powders used are given in Table 1.

Two different steels coupons of dimensions 150x30x2 mm were used as substrates. Half of the coatings was sprayed on AISI 304 stainless steel samples. The rest of the layers was obtained on C45 (EN 1.11191) high grade steel coupons. Both substrates compositions are given in Table 2.

2.2. Coatings deposition

The coatings were obtained using a Sulzer Metco model F4-MB air plasma spray gun mounted on an industrial robot. Before spraying, the substrate was blasted with corundum grit and cleaned with ethanol to remove any dust or grease residue from the surface. In the case of alumina-titania coatings, a Ni-Al metallic alloy was sprayed between steel substrate and ceramic coating in order to improve adhesion. It was also necessary to hold the substrate temperature between 95 and 200 ºC throughout the process in order to avoid spalling during the final cooling. In contrast, tungsten carbide coatings displayed very good adhesion without requiring the presence of a bond coat nor preheating of the substrate.

The main spraying parameters are given in Table 3. Tungsten carbide coatings were sprayed using Ar/H_2 or Ar/He mixtures as plasma-forming gases with a view to studying the effect of the nature of the secondary gas on the characteristics of the resulting coatings. In the case of the ceramic coatings, this paper describes only the influence of the feeding powder particle size and of substrate nature. The effect on some spraying parameters on coating microstructure and properties has been reported elsewhere [32].

2.3. Characterization techniques

Coatings crystalline phases were evaluated by X-ray diffraction (XRD) techniques (Bruker D8). Then coatings cross-sections were observed by scanning electron microcopy (FEI Quanta 200F Field Emission Gun-SEM or JEOL 6300) connected to X-ray energy dispersion microanalysis equipments (EDX). Vickers microhardness values were determined by realizing 10 indentations with a charge of 200 g for 15 s using a LECO M400 microhardness tester. All measurements were made on polished cross-sections.

3. Results and Discussion

3.1. Characterization of WC-Co coatings

3.1.1. Microstructure analysis

APS deposition is a high energy technique, as a consequence the initial WC-Co powder is not only fused during the process but also it may undergo reactions such as decarburization or oxidation which can lower the mechanical properties of the deposited coating [33-35]. The XRD analysis of as-sprayed cemented carbides coatings obtained with both conventional and nanostructured powders, sprayed either with Ar/H_2 or Ar/He, showed the presence of tungsten carbide (WC), ditungsten carbide (WC_2) and traces of cobalt oxide (Figure 1).

It was found that coatings sprayed on both types of substrates present similar phase composition but the layers deposited on C45 display a much lower decomposition, as visible through weaker W_2C and W peaks in XRD spectra (Fig. 1). This effect is more important in the case of the nanostructured powder. This lower decomposition is probably due to the higher thermal conductivity of high grade C45, which allows a quicker cooling of the as sprayed coatings.

Moreover, coatings obtained using helium as secondary gas show lower decomposition than coatings sprayed with hydrogen: XRD spectra exhibit stronger WC peaks and lower W_2C and W peaks (Fig. 1). This can be explained by the lower energy of the plasma plume when helium is used as secondary gas and by the much higher gas flow rates which allow a higher plasma density and make difficult the entrance of oxygen inside the flame.

Finally, the substitution of conventional powders with agglomerated, nanostructured powders in APS process produced practically no changes in the XRD spectra, in most of the spraying conditions. However it was found that the nanostructured coating sprayed with helium on C45 high grade steel present a slightly lower decomposition than their conventional counterpart.

SEM micrographs have shown that all the coatings show a similar microstructure as can be observed in Figure 2 and 3 for conventional and nanostructured coatings respectively.

All coatings are highly heterogeneous with a porous splat-like structure. Three different zones were identified. First, the coatings have a matrix (referenced as A in Fig. 2 and 3) containing Co, W, and C in quantities that fluctuate throughout the layer, depending on temperature and decarburization levels. Furthermore, elemental tungsten phase is probably present in the vicinity of the splat boundary in areas of high W concentration (referenced as C). Finally fine dispersions of WC crystals in a cobalt-rich matrix are found in the zones referenced as B. Higher magnification of those areas are given in

Figure 4 in the case of the coatings deposited on C45 substrate using helium as secondary gas.

Although the microstructures of all coatings are quite similar, it was found that the WC crystals are much smaller when the coating is obtained from the nanostructured powders (figure 4). It was also observed that the coatings obtained from helium have a higher proportion of fine dispersion of WC crystals and contain less tungsten-rich white particles. These observations agree with the XRD results (Figure 1), which indicate a lower decomposition of the initial powder when spraying is done with helium.

Moreover, a recrystallization of small carbides from the melted matrix was observed in all coatings. This phenomenon becomes more important when the decomposition of the initial carbides increases. As can be seen in Figure 5, in the case of conventional coatings sprayed with hydrogen on C45 substrate, some of the initial WC crystals are partly melted in the surrounding matrix during the deposition process. Tungsten carbides (WC o and/or W_2C) crystallized from the matrix, giving rise to the formation of nanosized crystals, as the cooling is fast enough to avoid the growth of the newly formed crystals. The presence of such nanocrystals may influence the coating properties.

3.1.2. Microhardness measurement

The Vickers microhardness measurement data are detailed in Table 4. They show that there are no great differences between the conventional coatings and those obtained from the nanostructured powder. In contrast, the coatings sprayed with helium exhibit higher microhardness than those obtained using hydrogen as a secondary gas. It can be seen that the coatings obtained on the high grade steel substrate seem to present slightly higher microhardness value. However, these differences are not significant, if the experimental error is taken into account.

3.1.3. Discussion

As mentioned in the introduction, WC-Co coatings are commonly used as wear resistant coatings. Although, further mechanical characterization comprising fracture toughness measurement and wear resistance determination is currently in progress, the microstructure characterization already give an idea of which coatings should give the best behavior.

First, microstructural characterization reveals an important decomposition of WC crystals during the projection with the appearance of new phases (W_2C and W). In fact, significant differences exist between the crystalline phases of the powder and the crystalline phases of the coating. During deposition, WC crystals undergo a partial decomposition, possibly as results of parallel reactions which involve both carbon and tungsten:

$$WC \rightarrow C + W$$

$$C + O_2 \rightarrow CO_2\uparrow$$

$$W + WC \rightarrow W_2C$$

Such decarburization occurs in all coatings and does not depend on the powder particles size. However, it can be significantly reduced using an Ar/He mixture to form the plasma instead of the usual Ar/H_2 mixture, due to a lower plasma temperature and higher gas flow rates which reduce the quantity of oxygen present in the plasma plume. Moreover, it was found that coatings sprayed on AISI 304 stainless steel present a higher decomposition than layers deposited on C45 high grade steel, as a consequence of the much higher thermal conductivity of C45 substrate which allows higher cooling rate of the coating and reduces available time for decomposition.

It is important to point out that the decomposition of the tungsten carbides during projection is highly prejudicial to the coatings properties. Actually, many investigators have studied this decomposition, and have tried to minimize it in order to obtain

coatings with enhanced mechanical and tribological properties [33-35]. In effect, the presence of W_2C and elementary W as well as the disappearance of the WC initial crystals is detrimental to the wear resistance of such layers. As a consequence, coatings sprayed with helium should present better tribological properties than coatings deposited with hydrogen as a result of their lower decarburization. For the same reason, the wear resistance is expected to be higher when the coatings are sprayed on C45 high grade steel instead of AISI 304 stainless steel.

Finally, no great differences were observed in the crystalline phases present in the coatings obtained from different powders. Nevertheless, SEM observation reveals that the main difference between nanostructured and conventional coatings resides in the size of the tungsten carbides crystals which are much smaller in the second case. It is expected that reducing the size of the carbides should enhance the coating wear resistance but it should be confirmed by tribological testing.

3.2. Characterization of Al_2O_3-TiO_2 coatings

3.2.1. Microstructure analysis

In the case of the ceramic coatings, XRD analysis (Figure 6) showed that the main phases were α-Al_2O_3 (corundum), γ-Al_2O_3, and TiO_2 (rutile) when the starting powders essentially contained α-Al_2O_3. ~~When the powder is heated in the plasma flame, γ-alumina forms. Then, as the particles cool down, part of the γ-Al_2O_3 transformed back to corundum.~~ In general, the layers deposited on C45 substrate present a lower α- to γ-alumina ratio than the coatings sprayed on AISI 304. This is probably due to a higher cooling rate of these coatings because of the higher thermal conductivity of C45 steel. Furthermore, the nanostructured coatings exhibited a larger α- to γ-alumina ratio than the conventional coatings, as shown in Figure 6. In fact the nanostructured powder is formed by porous agglomerates of nanoparticles [32] and, as a consequence has a low thermal conductivity, avoiding the complete fusion of the granulates. Actually, part of

the initial corundum does not transform to γ-alumina, and remains in the final coating, as confirmed by the SEM observations below.

Typical micrographs can be seen in Figure 7 and 8 for the conventional (left) and nanostructured (right) coatings in the case of AISI304 and C45 substrate respectively. EDX analysis was performed to determine the atomic composition of the different phases found in the coatings. Comparing these results with those of XRD analysis, the likely phase composition of each zone in the coating microstructure could be deduced. Both nanostructured and conventional coatings are confirmed to be formed by a completely melted matrix of γ-Al_2O_3 with dissolved Ti+4 (marked A and D in Fig. 7 and 8) containing clear splat-like particles with high TiO_2 content (marked B and E). In the case of the nanostructured coatings, agglomerate-like particles (marked F), corresponding to partially melted starting agglomerates were observed. Due to these uncompleted melting zones, α- to γ-alumina ratio is higher in the nanostructured coating as mentioned above. This microstructural description, which has been set out elsewhere [23,24] was observed on both substrates.

Finally, EDX analysis of the different phases showed a major difference between conventional and nanostructured coatings. Although both coatings have a similar matrix composition, conventional coatings present a segregation of titanium in the white zones which showed a lower aluminum content and much higher titanium proportion. In the nanostructured coating, however, the white zones have in general similar concentration of aluminium than the matrix with slightly higher titanium content. This segregation has been also pointed out in previous works [32,36].

3.2.2. Microhardness measurement

The results of the microhardness measurements are given in Table 5. When the error in the resulting values (5–10%) is taken into account, it appears that the nanostructured coatings display a higher microhardness than their conventional counterparts.

Moreover, it was found that the layers deposited on AISI 304 substrates present higher microhardness than the layers sprayed on C45.

3.2.3. Discussion

Microstructure characterization have shown that the main crystalline phases found in the coatings are α-Al_2O_3 (corundum) and γ-Al_2O_3, whereas feeding powders are mainly formed by α-Al_2O_3. The origin of α- and γ-Al_2O_3 in plasma sprayed alumina coatings was explained by McPherson [37]. This author have shown that, when a particle is completely melted by the plasma plume, γ-Al_2O_3 nucleates preferably from the liquid phase. In fact, γ-Al_2O_3 has a lower interfacial energy with the liquid which compensates for the low driving force for crystallization resulting from the small free energy difference between liquid and crystalline phases. Occasionally, if the cooling rate is sufficiently slow, α-Al_2O_3 may appear. However, most of the α-phase present in the coating originates from unmelted of partially melted particles. In the later case, unmolten α-Al_2O_3 acts as a nuclei for crystallization, favoring the formation of corundum during cooling.

It is important to point out that nanostructured coatings display a greater relation of α- to γ- alumina than the conventional layers, independently of the substrate. Actually, in the nanostructured case, SEM observation have shown a bimodal microstructure formed by partially molten agglomerates embedded in a completely fused matrix.

Indeed, during the deposition of nanostructured powders, it is important to achieve a partial fusion of the initial powder in order to avoid excessive grain growth and to preserve part of the nanostructure in the coating. A_2O_3-TiO_2 nanostructured feedstock is formed by porous agglomerates, with a low thermal conductivity. Therefore, particles are not completely molten during spraying and part of the initial α-Al_2O_3 is retained in the deposited layer.

A typical application of Al_2O_3-TiO_2 coatings are wear resistant layers. Wear resistance of the coatings sprayed on AISI 304 stainless steel have been reported elsewhere by the authors [32]. The results showed that the nanostructured coatings present better properties than their conventional counterparts, as a consequence of the main microstructural differences existing between both coatings.

First, the presence of partially fused agglomerates in the nanostructured layer can slow down the propagation of cracks inside the coating as they should present higher fracture toughness than that of the matrix [38]. Then, in the case of conventional coatings, segregation of titanium at the splats boundaries was observed whereas a uniform repartition of titanium was found in the nanostructured coating. As titanium segregation leads to greater delamination, it reduces the wear resistance of the conventional layers [23]. As a consequence, nanostructured coatings exhibit better tribological properties.

Tribological characterization is still in progress on the coating sprayed on C45 steel. It is important to point out that the microstructure is quite independent of the substrate nature. As a consequence, it is expected that the nanostructured layers display better wear resistance than their conventional counterpart. However, XRD analysis revealed differences in the α- to γ-alumina ratio. Thus, the tribological behavior may be slightly different.

4. Conclusions

In order to obtain nanostructured coatings by thermal spraying, reconstituted nanostructured powder (agglomerates made up of nanoparticles) is needed. Though different methods for obtaining nanoparticles are available, effective nanoparticle agglomeration is mainly performed by spray drying.

In this study, WC-Co and Al_2O_3-TiO_2 coatings were obtained by atmospheric plasma spraying using reconstituted nanostructured powders. In the WC-Co coatings,

significant decomposition of the WC particles occurred during spraying and new phases (W_2C and W) appeared. This decarburization which is prejudicial to wear resistance, decreased when helium was used as spraying gas.

At microstructural level, the nanostructured Al_2O_3-TiO_2 coatings exhibited a fused matrix of γ–Al_2O_3 and Ti^{4+}, which contained partly fused areas that retained the initial nanostructure of the powder. The presence of these areas may explain the higher microhardness of these coatings compared with that of their conventional counterparts obtained from micrometric powders and leads to better tribological properties.

Acknowledgements

This work has been conducted by support of the Spanish Ministery for Sciences and Innovation (Project: MAT2006-12945-C03).

References

1. H. Gleiter, “Nanostuctured Materials: Basic Concepts and Microstructure”, Acta Mater., **48**, 1-29 (2002).
2. E. Roduner, “Size Matters: Why Nanomaterials are Different”, Chem. Soc. Rev., **35**, 583-592 (2006).
3. M. Gell, “Application Opportunities for Nanostuctured Materials and Coatings”, Mater. Sci. Eng. A, **204**, 246-251 (1995).
4. N.B. Dahotre, and S. Nayak, “Nanocoatings for Engine Application”, Surf. Coat. Technol., **194**, 58-67 (2005).
5. J.R. Davis (ed.), Handbook of Thermal Spray Technology, Materials Park: ASM, 2004.
6. R.B. Heimann, “Applications of Plasma-Sprayed Ceramic Coatings”, Key Eng. Mater., **122-124**, 399-442 (1996).
7. J. He, and J.M. Schoenung, “A Review on Nanostructured WC-Co Coatings”, Surf. Coat. Technol., **157**, 72-79 (2002).

8. E.P. Song, J. Ahn, S. Lee and N.J. Kim, “Microstructure and Wear Resistance of Nanostructured Al_2O_3-8wt.%TiO_2 Coatings Plasma-Sprayed with Nanopowders”, Surf. Coat. Technol., **201**, 1309-1315 (2006).

9. C.P. Poole and F.J. Owens, Introduction to Nanotechnology, Hoboken (New Jersey): Wiley, 2003.

10. G. Cao, Nanostructures & Nanomaterials: Synthesis, Properties & Applications, London: Imperial College Press, 2004.

11. N. Eigen, F. Gärtner, T. Klassen, E. Aust, R. Bormann and H. Kreye, “Microstructures and Properties of Nanostructured Thermal Sprayed Coatings Using High-Energy Milled Cermet Powders”, Surf. Coat. Technol., **195**, 344-357 (2005).

12. D. Vie, E. Martínez, F. Sapiña , J.V. Folgado and A. Beltrán, “Freeze-Dried Precursor-Based Synthesis of Nanostructured Cobalt-Nickel Molybdates Co1-xNixMoO4”, Chem. Mater., **16**, 1697-1703 (2004).

13. J. Karthikeyan, C.C. Berndt, J. Tikkanen, S. Reddya and H. Herman, “Plasma Spray Synthesis of Nanomaterial Powders and Deposits”, Mater. Sci. Eng. A, **238**, 275-286 (1997).

14. Y.C. Zhu, C.X. Ding, K. Yukimura, T. Xaio and P.R. Strutt, “Deposition and Characterization of Nanostructured WC-Co Coating”, Ceram. Int., **27**, 669-674 (2001).

15. X. Lin, Y. Zeng, S.W. Lee and C. Ding, “Characterization of Alumina -3wt% Titania Coating Prepared by Plasma Spraying of Nanostructured Powders”, J. Eur. Ceram. Soc., **24**, 627-634 (2004).

16. X. Lin, Y. Zeng, X. Zhou and C. Ding, “Microstructure of Alumina–3wt.% Titania Coatings by Plasma Spraying with Nanostructured Powders”, Mater. Sci. Eng. A, **357**, 228-234 (2003).

17. X.Q. Cao, R. Vassen, S. Schwartz, W. Jungen, F. Tietz and D. Stöever, “Spray-Drying of Ceramics for Plasma-Spray Coating”, J. Eur. Ceram. Soc., **20**, 2433-2439 (2000).

18. Y.C. Zhu, C.X. Ding, K. Yukimura, T. Xaio and P.R. Strutt, “Deposition and Characterization of Nanostructured WC-Co Coating”, Ceram. Int., **27**, 669-674 (2001).

19. R.S. Lima and B.R. Marple, “Thermal Spray Coatings Engineered from Nanostructured Ceramic Agglomerated Powders for Structural, Thermal Barrier and Biomedical Applications: a Review”, J. Therm. Spray Technol., **16**, 40-62 (2007).

20. Y. Zeng, S.W. Lee, and C.X. Ding, “Plasma Spray in Different Nanosize Alumina”, Mater. Lett., **57**, 495-501 (2002).

21. N. Berger-Keller, G. Bertrand, C. Filiare, C. Meunier and C. Coddet, “Microstructure of Plasma-Sprayed Titania Coatings Deposited from Spray-Dried Powder”, Surf. Coat. Technol., **168**, 281-290 (2003).

22. S.O. Chwa, D. Klein, F.L. Toma, G. Bertrand, H. Liao, C. Coddet and A. Ohmori, “Microstructure and Mechanical Properties of Plasma Sprayed Nanostructured TiO2–Al Composite Coatings”, Surf. Coat. Technol., **194**, 215-224 (2005).

23. J. Ahn, B. Hwan, E.P. Son, S. Lee, and N.J Kim, “Correlation of Microstructure and Wear Resistance of Al_2O_3-TiO_2 Coatings Plasma Sprayed with Nanopowders”, Metall. Mater. Trans. A, **37**, 1851-1861 (2006).

24. E.H. Jordan, M. Gell, Y.H. Sohn, D. Goberman, L. Shaw, S. Jiang, M. Wang, T.D. Xiao, Y. Wang and P. Strutt, “Fabrication and Evaluation of Plasma Sprayed Nanostructured Alumina-Titania Coatings with Superior Properties”, Mater. Sci. Eng.,A, **301**, 80-89 (2001).

25. Y. Yang, Y. Wang, Z. Wang, G. Liu and W. Tian, “Preparation and Sintering Behaviour of Nanostructured Alumina/Titania Composite Powders Modified with Nano-Dopants”, Mater. Sci. Eng. A, **490**, 457-464 (2008).

26. H. Chen and C.X. Ding, “Nanostructured Zirconia Coating Prepared by Atmospheric Plasma Spraying”, Surf. Coat. Technol., **150**, 31-36 (2002).

27. C. Zhou, N. Wang and H. Xu, “Comparison of Thermal Cycling Behavior of Plasma-Sprayed Nanostructured and Traditional Thermal Barrier Coatings”, Mater. Sci. Eng., **452-453**, 569-574 (2007).

28. Y. Zeng, S.W. Lee, L. Gao and C.X. Ding, “Atmospheric Plasma Sprayed Coatings of Nanostructured Zirconia”, J. Eur. Ceram. Soc., **22**, 347-351 (2002).

29. Y.C. Zhu, K. Yukimura, C.X. Ding, and P.Y. Zhang, "Tribological Properties of Nanostructured and Conventional WC-Co Coatings Deposited by Plasma Spraying", Thin Solid Films, **388**, 277-282 (2002).

30. M.D Salvador, V. Amigó, F. Segovia, J. Candel, V. Bonache, E. Sánchez and V. Cantavella, "Comportamiento al Desgaste de Recubrimientos de WC Proyectados por Plasma a partir de Polvos Micro y Nanoestructurados", Rev. Metal. Madrid, **44**, 222-232 (2008).

31. Y.C. Zhu, C.X. Ding, K. Yukimura, T. Xaio and P.R. Strutt, "Deposition and Characterization of Nanostructured WC-Co Coating", Ceram. Int., **27**, 669-674 (2001).

32. E. Sánchez, V. Cantavella, E. Bannier, M. D. Salvador, F. Segovia, J. Morgiel, J. Grzonka, A. Boccaccini, "Deposition of Al_2O_3-TiO_2 Nanostructured Powders by Atmospheric Plasma Spraying", J. Therm. Spray Technol., **17**, 329-337 (2008).

33. C.Verdon, A.Karimi &J.L. Martin, "A study of high velocity oxy-fuel thermally sprayed tungsten carbide based coatings. Part 1: Microstructures", Materials Science and Engineering, **A246**, 11-24 (1998).

34. C.J. Li, "Effect of powder structure on the structure of thermally sprayed WC-Co coatings", Journal of materials science **32**, 785-794 (1996).

35. M.E. Vinayo et al., "Plasma sprayed WC–Co coatings: Influence of spray conditions (atmospheric and low pressure plasma spraying) on the crystal structure, porosity, and hardness", Journal of Vacuum Science and Technology A: Vacuum, Surfaces, and Films, **3** (6), 2483-2489 (1985).

36. X. Lin, Y. Zeng, S.W. Lee and C. Ding, "Characterization of Alumina -3wt% Titania Coating Prepared by Plasma Spraying of Nanostructured Powders", J. Eur. Ceram. Soc., **24**, 627-634 (2004).

37. R. McPherson, "On the formation of thermally sprayed alumina coatings", J. Mater. Sci., **15**, 3141-3149 (1980).

38. P. Bansal, N.P. Padture, and A. Vasiliev, “Improved interfacial mechanical properties of Al_2O_3-13wt%TiO_2 plasma-sprayed coatings derived from nanocrystalline powders”, Acta Mater., **51,** p 2959-2970 (2003).

Tables

Table 1. Commercial feeding powders characteristics (supplier data).

	WC-Co		Al_2O_3-TiO_2	
	Conventional	Nanostructured	Conventional	Nanostructured
Manufacturer	Sulzer Metco	Inframat Advanced Materials	Sulzer Metco	Inframat Advanced Materials
Reference	METCO 72F NS	Infralloy™ S7412	METCO 130	Nanox™ S2613S
Composition	WC-Co (weight ratio 88:12)		Al_2O_3-TiO_2 (weight ratio 87:13)	
Additives	-	-	-	$CeO;ZrO_2$
Particle size	-	50–500 nm	-	50–500 nm
Agglomerate size	15–45 μm	5–45 μm	15–53 μm	30 μm

Table 2. Chemical composition of the steel substrates.

	C wt%	Mn wt%	Si wt%	Cr wt%	Ni wt%	P wt%	S wt%	Mo wt%	Al wt%	Fe
AISI 304	0.08	2	0.75	18	10	0.045	0.03	-	-	balance
C45	0.458	0.717	0.02	0.059	0.062	0.008	0.01	0.003	0.051	balance

Table 3. Main plasma spraying parameters.

Material	Ar (slpm)	H_2 (slpm)	He (slpm)	Intensity (A)	Spraying distance (mm)	Flow rate (g/min)
WC-Co	65	3	-	750	130	50
	60	-	120	625	110	30
Ni-Al (bond coat)	45	11	-	600	140	80
Al_2O_3-TiO_2	35	12	-	600	120	45

slpm = standard litre per minute

Table 4. Vickers microhardness of WC-Co plasma-sprayed coatings.

		WC-Co coatings			
Substrate nature		AISI 304		C45	
Plasma gas nature		Ar/H_2	Ar/He	Ar/H_2	Ar/He
HV GPa	Conventional	6.1 ± 0.2	7.4 ± 0.7	6.6 ± 0.3	7.6 ± 0.3
	nanostructured	6.6 ± 0.7	7.6 ± 0.7	7.2 ± 0.3	8.1 ± 0.7

Table 5. Vickers microhardness of Al_2O_3-TiO_2 plasma-sprayed coatings.

		Al_2O_3-TiO_2 coatings	
Substrate nature		AISI 304	C45
HV GPa	**Conventional**	7.6 ± 0.3	6.3 ± 0.6
	nanostructured	8.4 ± 0.4	7.0 ± 0.4

Figures captions

~~Figure 1. Coating formation by thermal spraying [6].~~

~~Figure 2. Classification of thermal spray techniques [5].~~

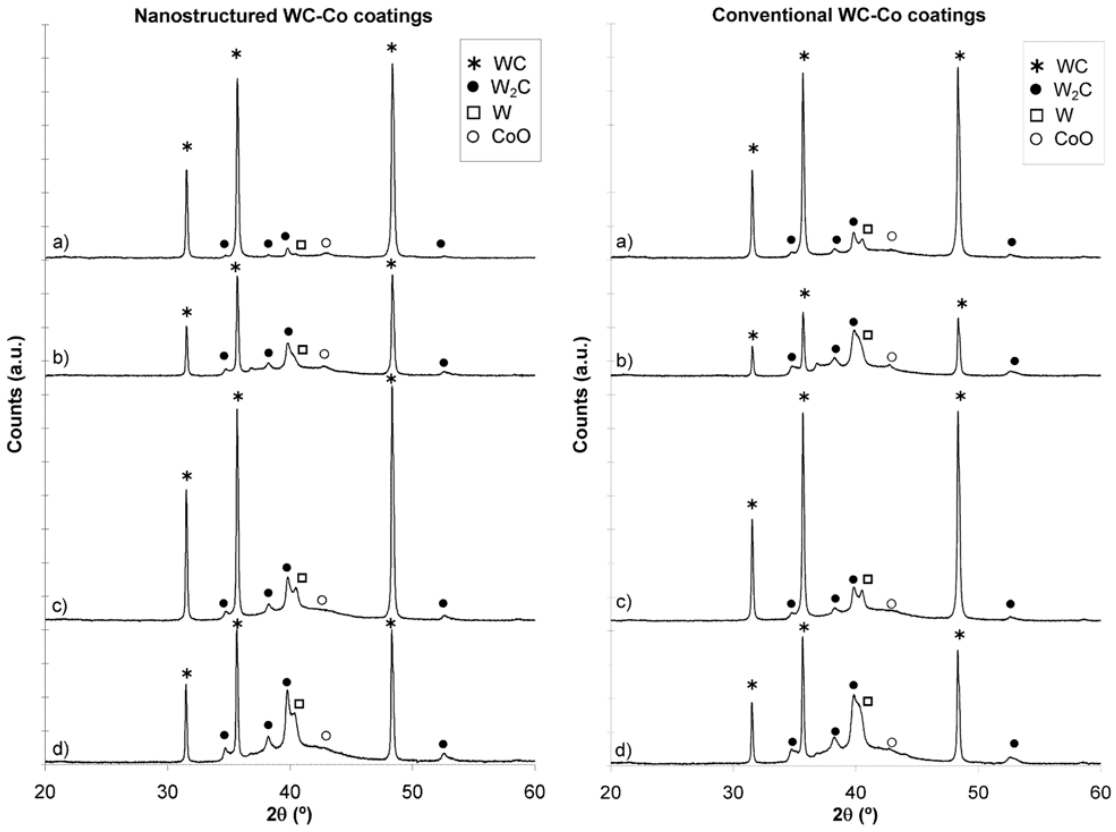

Figure 1. XRD diffraction patterns of WC-Co coatings sprayed a) on C45 steel with Ar/He, b) on C45 steel with Ar/H_2, c) on AISI 304 steel with Ar/He, d) on AISI 304 steel with Ar/H_2.

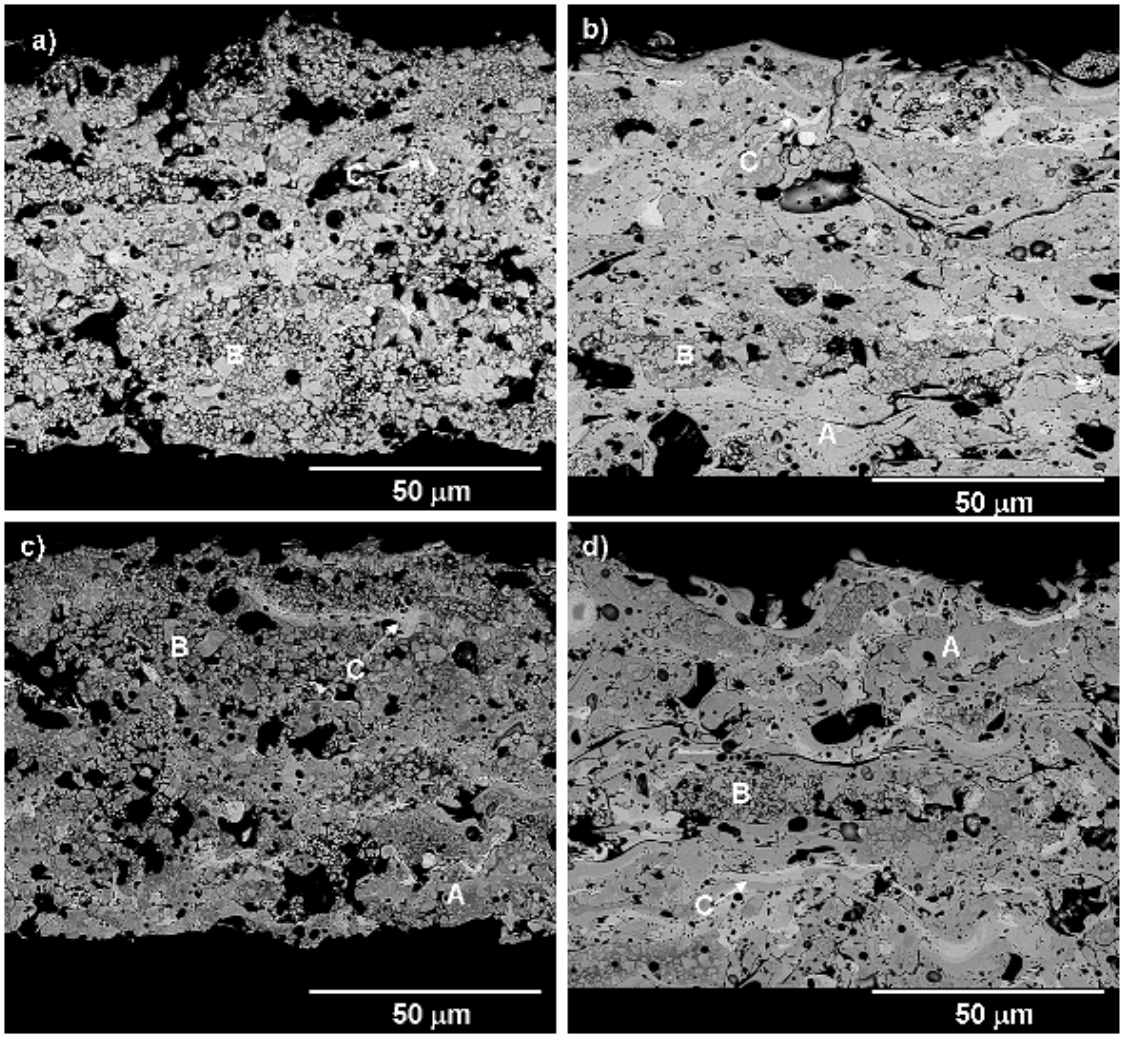

Figure 2. SEM micrographs of WC-Co conventional coatings sprayed a) on C45 steel with Ar/He, b) on C45 steel with Ar/H_2, c) on AISI 304 steel with Ar/He, d) on AISI 304 steel with Ar/H_2.

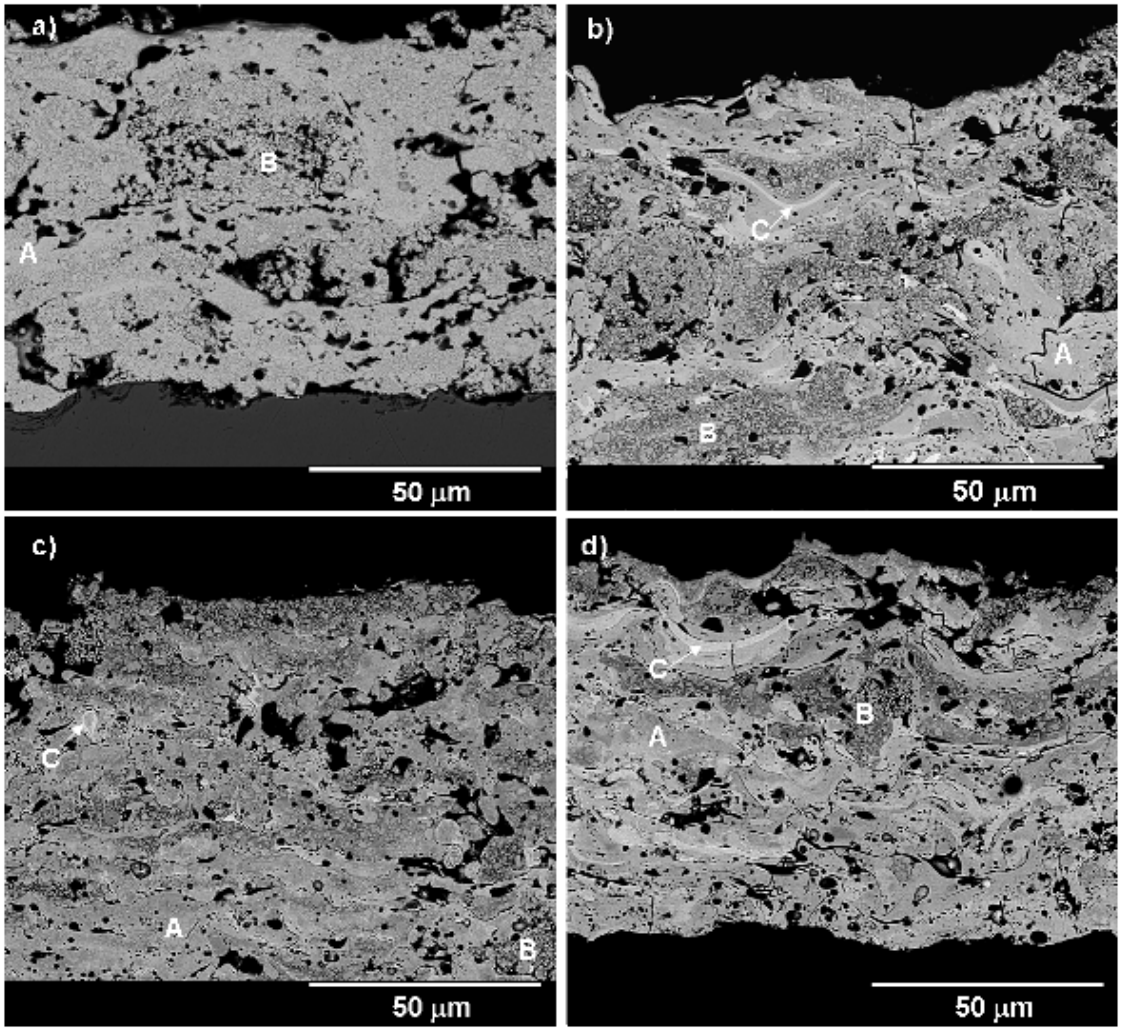

Figure 3. SEM micrographs of WC-Co nanostructured coatings sprayed a) on C45 steel with Ar/He, b) on C45 steel with Ar/H_2, c) on AISI 304 steel with Ar/He, d) on AISI 304 steel with Ar/H_2.

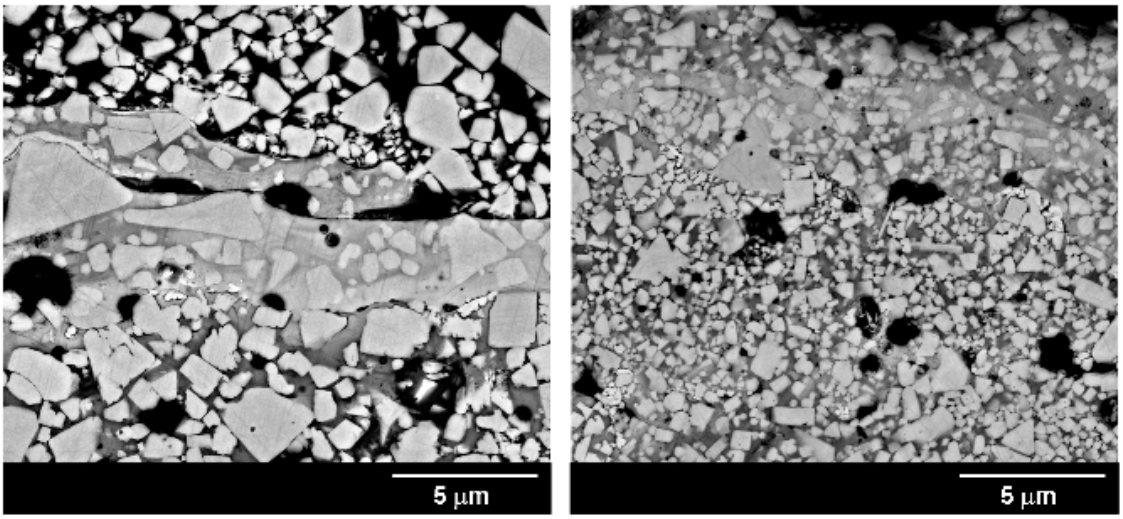

Figure 4. SEM micrographs of WC-Co conventional (left) and nanostructured (right) coatings sprayed on C45 steel with Ar/He at high magnification (areas referred as B in figure 4 and 5).

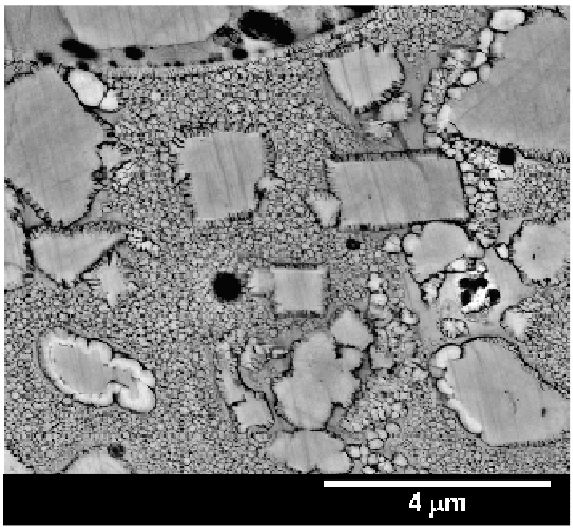

Figure 5. SEM micrographs of WC-Co conventional coatings sprayed on C45 steel with Ar/He at high magnification showing the nanocrystals formed during cooling.

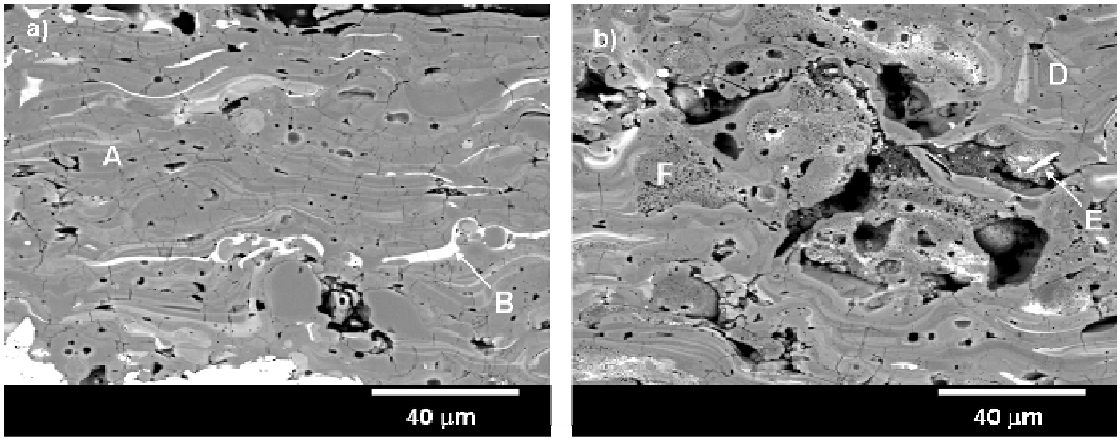

Figure 6. XRD diffraction patterns of Al_2O_3 coatings sprayed a) on C45 steel, b) on AISI 304 steel.

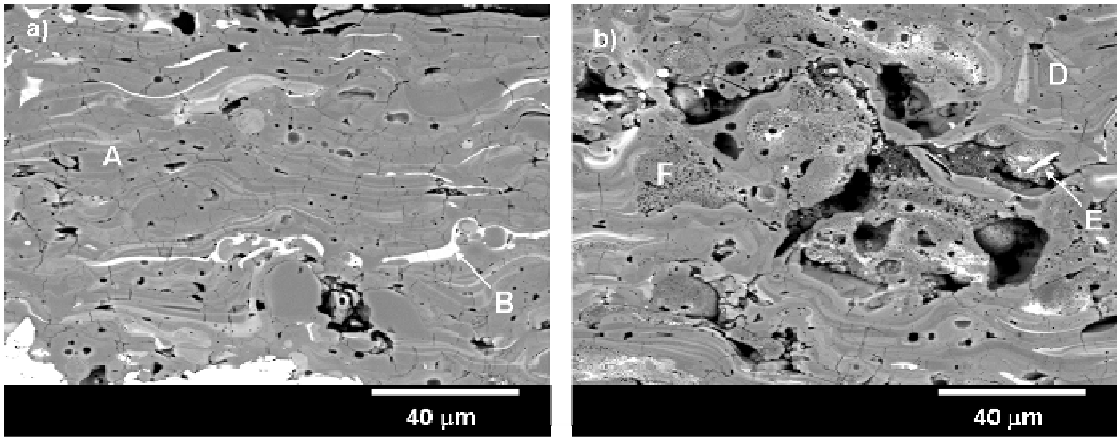

Figure 7. SEM micrographs of conventional (left) and nanostructured (right) Al_2O_3 coatings sprayed on AISI 304 steel.

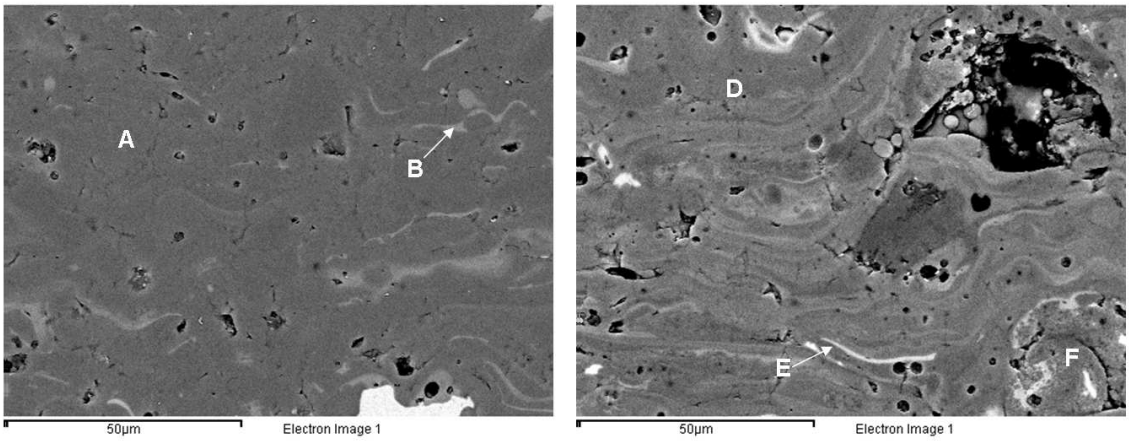

Figure 8. SEM micrographs of conventional (left) and nanostructured (right) Al_2O_3 coatings sprayed on C45 steel.